Journal of Materials and Environmental Science
ISSN : 2028-2508
e-ISSN : 2737-890X
CODEN : JMESCN

J. Mater. Environ. Sci., 2023, Volume 14, Issue 03, Page 360-372

http://www.jmaterenvironsci.com

Modeling of Multi-Layered Heat Transfer for Investigating Thermal Performance of a Refrigerator Powered with Solar Energy

Ajayi A.B[1], Sobamowo M.G.[2], Nnadi I.[3], Oladosu S. A.[4]

[1,2,3]Department of Mechanical Engineering, Faculty of Engineering, University of Lagos, Akoka, Yaba, Lagos. Nigeria.
[4]Department of Mechanical Engineering, Faculty of Engineering, Lagos State University, Epe Campus, Lagos. Nigeria
[1]Corresponding author, Email address: abajayi@unilag.edu.ng
[2]Corresponding author, Email address: gsobamowo@unilag.edu.ng

Received *15 Feb 2023,*
Revised *25 Mar 2023,*
Accepted *27 Mar 2023*

Citation*: Ajayi A. B., Sobamowo, M. G.., Nnadi, I., (2023) Modeling of Multi-Layered Heat Transfer for the Investigation of Thermal Performance of a Refrigerator Powered with Solar Energy, J. Mater. Environ. Sci., 14(3), 360-372.*

Abstract: Two-dimensional thermal models for the heat conductions through composite walls of a refrigerator was developed for the investigation of thermal performance of a refrigerator powered with solar energy. A refrigerating system was developed locally where the ambient temperature is higher than the ambient temperature in temperate regions where imported refrigerating systems is normally manufactured. This developed refrigerating system unit needs to be investigated on how to improve its performance in tropical region. Finite difference method was used to solve the developed equations numerically. The performance of the system under different ambient temperature was simulated for the composite walls. The installation, testing and performance evaluations were successfully carried out. It was concluded from the numerical simulation results that the performance of the refrigerator was dependent on the ambient temperature, convective heat transfer coefficient, thicknesses of the composite walls, the insulating materials, thermal property of the wall component and the insulating material used for the construction of the refrigerator.

Keywords: *Heat transfer; Refrigeration System; Finite Difference Method (FDM); Solar Energy*

1. Introduction

The ever-increasing energy demands, growing energy cost and gradual depletion of fossil fuel coupled with the environmental threats accompanying the utilization of fossil fuel for energy generation has been the driving forces behind generation and utilization of energy sources that are renewable such as solar energy. Nigeria is a country with a population of over 200 million people, with less than 50% of its population having good access to the National Grid for their electricity supply needs (Ren and Ogura (2021); Hafeez *et al.* (2022)). City dwellers have higher percentage of accessibility to electricity. Meanwhile, rural dwellers, which constitute more than 70% of Nigeria population of more than 200 million people have less access to national grid electricity. The rural areas, with higher population, do not have easy access to fossil fuels and other energy resources. Thus, the power required to run their vapour-compression refrigerators are either too costly to acquire or not readily available particularly in the remote areas where they are used for the preservations of their agricultural produce.

Various researchers had worked on different types of technologies for powering refrigerators for different applications. Harvey (1990) studied a version of the regenerative solar refrigerator cycle and appraised a 1-ton/day refrigerator for use in the Zambia. He was of the opinion that the technology was

more energy efficient but was restricted by its bulky size and that its moving parts will need constant maintenance. Iloeje (1977) developed and tested experimentally, ammonia-calcium chloride system in Nigeria but did not produce it commercially. Saunier and Reddy (1986) designed and developed a biomass fuelled device in Thailand. Neither Iloeje (1977) or Saunier and Reddy (1986) system was developed commercially. Ahmed, *et. al.* (1986) investigated a continuous ammonia-water refrigeration system in Sudan. They used electricity to drive the feed pump. There were many technical difficulties that prevented successful operation of the project. Hinotani (1986) designed, constructed and tested a solar diffusion absorption refrigerator (SDR). The refrigerator design was a success and the pumping rate of the solution was close to the optimum value over the whole range of refrigerating temperatures. But the hydrogen flow rate was the challenge which led to the ammonia generated being poorly evaporated with overall Coefficient of Performance (COP) of less than 0.05. Ewert et al (1998) experimented with a solar PV refrigerator using Thermoelectric, Stirling and vapour compressor heat pumps. Mohamed and Samuel (2007) designed, fabricated and carried out economic evaluation of vapour compression refrigeration system powered by solar photovoltaic (SPV) to obtain conditions favourable for storing potato in different operating scenarios. Aktacir (2011) studied experimentally a multi-purpose PV-refrigeration unit. Kim and Ferreira (2008) reviewed different types of solar refrigerating units concentrating on the usefulness of each technology in providing sustainable solutions. It was pointed out that one of the advantages of powering refrigeration with solar panels is its simplicity in construction and high efficiency when used in conjunction with a normal vapour compression refrigeration unit. After the critical review of the literature, it can be inferred that the photovoltaic unit applications are the most preferred solar system in the refrigeration systems (Ewert, et al, 1998) (Kim and Ferreira, 2008). Midani, et. al (2020) studied an experimental performance of thermoelectric refrigerator using fan and without fan is presented. The result shows that the cold side temperature decreases from 25.5 degree C to -5 degree C for 37 watt (with fan) and 25.5 degree C to -7.5 degree C for 37-watt without fan. Lawal and Chang (2021) developed a cooler box cooling system with a low power supply and evenly distributed temperature for food storage that adopted both conduction and convection heat transfer to solve the problems. The cooler box is made of three-layer wall. The obtained results showed steady temperature distributions with time at various points of the layers including the cold and hot region. The cooling capacity changes and became steady with the time. The conductive heat transfer is the dominant of the total heat transfer (Qc). Biswas and Kandasamy (2021) fabricated solar thermoelectric cooler (STEC). They investigated the effect of varying input electric current on the cold side temperature of TEM, cooling capacity, power consumption and coefficient-of-performance (COP). Their results showed that the cold side temperature decreased to 5±0.2 ^{0}C in 120 and 180 min for without and with product load (0.5 kg fish fillets), respectively. The STEC could be considered as an alternate "green-option" to the domestic refrigerator where electricity is not accessible. Chavan *et al.* (2022) invented a mobile thermoelectric refrigeration system useful for marketing fruits and vegetables efficiently. The performance of their invention indicated notable results for physiological loss in weight, firmness, and colour values and overall acceptability of the crop. The system is discovered to be economical, has a higher coefficient of performance, and maintains the freshness and quality of perishable agricultural produce during marketing and transportation.

Sobamowo *et al* (2012) designed and developed a dual powered refrigerator using electricity from the national grid and solar power generated by photovoltaic panels. This system works on power from the grid system when there is supply of electricity and automatically switches to solar power whenever the national grid system fails. Deep cycle batteries system was incorporated into the unit to

store the charges generated to operate the system when the sun is down or when there is no solar insolation or no electricity from the grid. This refrigerating system was developed locally where the ambient temperature is higher than the ambient temperature in temperate regions where imported refrigerating systems is normally manufactured. However, this system needs to be investigated on how to improve its performance.

The objective of this paper is to develop a multi-layered heat transfer models for the investigation of the thermal performance of a refrigerator powered with solar energy that can be suited for tropical region.

2. Methodology

2.1 Heat Transfer Analysis of the Solar Refrigerating System

The solid body of the refrigerating system is made of composite rectangular walls. In order to develop the model for transient heat transfer through the composite walls, thermal model is developed for one wall starting from the first principle. This is achieved by assuming a rectangular wall as shown Figure 1a. Considered a volume of material of arbitrary shape in Figure 1b.

(a)

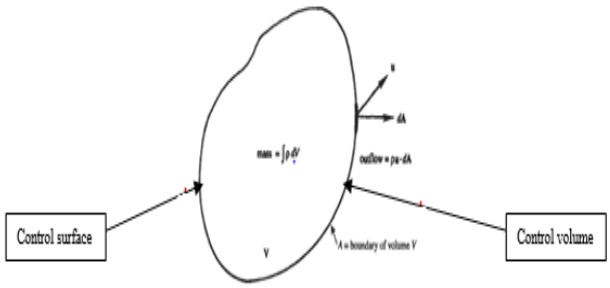

(b)

Figure 1a: The composite wall of the refrigerator**. Figure 1b:** The fixed control volume

The net heat flow across the boundary S of the volume V is given in **Eqn. 1**

Net heat transfer rate across the surface boundary = $\iint_S \vec{q}.\vec{n}.\mathrm{dS}$ **Eqn. 1**

The heat energy stored inside the control volume V is given as **Eqn. 2**

$$\iiint_V \frac{\partial\left(\rho c_p T\right)}{\partial t} dV \qquad \textbf{Eqn. 2}$$

The bulk motion in the control volume is given as **Eqn. 3**

$$\iiint_V \nabla.\left(\rho c_p u T\right) dV \qquad \textbf{Eqn. 3}$$

The rate of heat generation within the control volume is given as **Eqn. 4**

$$\iiint_V q_g dV \qquad \textbf{Eqn. 4}$$

It is required that for the heat energy to balance, the rate of energy flow into the storage within the control volume V should be equal to the difference between the rate at which heat is accumulated within the volume V, and the rate at which the heat energy is transferred across the boundary S. Hence, this is expressed in **Eqn. 5**

$$\iiint_V \frac{\partial\left(\rho c_p T\right)}{\partial t} dV + \iiint_V \nabla.\left(\rho c_p u T\right) dV = \iiint_V q_g dV - \iint_S \vec{q}.\vec{n}.\mathrm{dS} \qquad \textbf{Eqn. 5}$$

Eqn. 5 can be re-written to give **Eqn. 6** as

$$-\iint_S \vec{q}.\vec{n}.\mathrm{dS} + \iiint_V q_g dV = \iiint_V \frac{\partial\left(\rho c_p T\right)}{\partial t} dV + \iiint_V \nabla.\left(\rho c_p u T\right) dV \qquad \textbf{Eqn. 6}$$

By using Gaussian divergence theorem gives **Eqn. 7** as

$$\iint_S \vec{q}.\vec{n}.\mathrm{dS} = \iiint_V \nabla \cdot \vec{q} dV \qquad \textbf{Eqn. 7}$$

By substituting **Eqn. 7** into **Eqn. 6, Eqn. Eqn. 6** becomes **Eqn. 8** given as

$$-\iiint_V \nabla \cdot \vec{q} dV + \iiint_V q_g dV = \iiint_V \frac{\partial\left(\rho c_p T\right)}{\partial t} dV + \iiint_V \nabla.\left(\rho c_p u T\right) dV \qquad \textbf{Eqn. 8}$$

But heat transfer rate through the control volume is given as **Eqn. 9**

$$\vec{q} = -k\nabla T \qquad \textbf{Eqn. 9}$$

Substituting **Eqn. 9** into **Eqn. 8** and applying triple integration gives **Eqn. 10,** this is the generalized governing equation of the temperature as a function of space and time.

$$\nabla \cdot \left(k\nabla T\right) + q_g = \frac{\partial\left(\rho c_p T\right)}{\partial t} + \nabla.\left(\rho c_p u T\right) \qquad \textbf{Eqn. 10}$$

Figure 2 shows the composite walls of the refrigerating system.

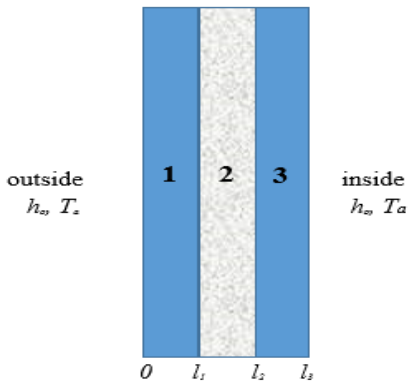

Figure 2: Composite walls of the refrigerating system

Figure 3a is the refrigerator walls' geometry.

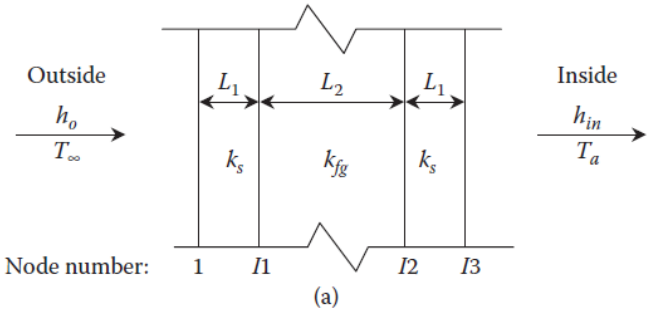

Figure 3a: Refrigerator walls' geometry

Eqn. 11 is

$$\nabla\cdot\left(k_i\nabla T_i\right)+q_{gi}=\frac{\partial\left(\rho_i c_{pi}T_i\right)}{\partial t}+\nabla.\left(\rho_i c_{pi}u_i T_i\right) \quad \text{where} \quad i=1,2,3 \qquad \textbf{Eqn. 11}$$

Since the wall is stationary and heat is not generated within the composite walls, **Eqn. 11** reduces to **Eqn. 12**

$$\nabla\cdot\left(k_i\nabla T_i\right)=\frac{\partial\left(\rho_i c_{pi}T_i\right)}{\partial t} \qquad \textbf{Eqn. 12}$$

If **Eqn. 12** is expanded for each of the walls, then, there will be an equation for each wall

Figure 3b is Steel Wall 1, boundary 1, that is outside air – steel interface

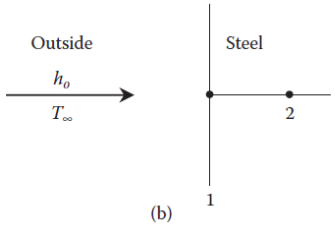

Figure 3b: Outside air–steel interface.

The transient heat conduction equation for **Figure 3b** is given by **Eqn. 13**

$$\nabla\cdot\left(k_1\nabla T_1\right)=\frac{\partial\left(\rho_1 c_{p1}T_1\right)}{\partial t} \qquad \textbf{Eqn. 13}$$

Figure 3c is Steel Wall 1, boundary 2, the left steel – insulation interface.

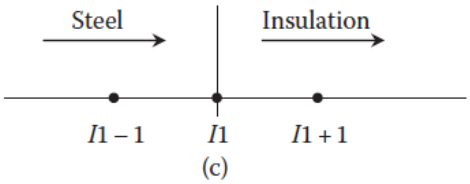

Figure 3c: Left steel–insulation interface.

The transient heat conduction equation for **Figure 3c** is given by **Eqn. 14**

$$\nabla\cdot\left(k_2\nabla T_2\right)=\frac{\partial\left(\rho_2 c_{p2}T_2\right)}{\partial t} \qquad \textbf{Eqn. 14}$$

Figure 3d is Steel Wall 2, boundary 3, the right insulation – steel interface

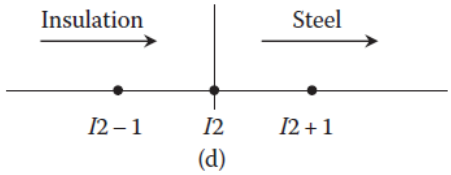

Figure 3d: Right insulation–steel interface.

The transient heat conduction equation for **Figure 3d** is given by **Eqn. 15**

$$\nabla\cdot\left(k_3\nabla T_3\right)=\frac{\partial\left(\rho_3 c_{p3}T_3\right)}{\partial t} \qquad \textbf{Eqn. 15}$$

Figure 3e is Steel Wall 2, boundary 4, the steel – inside air interface

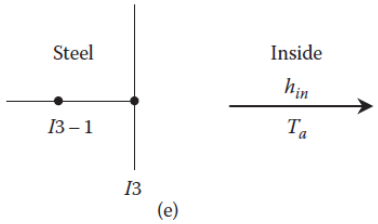

Figure 3e: Steel–inside air interface.

The transient heat conduction equation for **Figure 3e** is given by **Eqn. 15**

$$\nabla.\left(k_4\nabla T_4\right)=\frac{\partial(\rho_4 C_{p3}T_3)}{\partial t} \qquad \textbf{Eqn. 16}$$

The heat conduction within the walls (steel-insulation-steel) are given as a two-dimensional heat transfer analysis in the composite walls of rectangular coordinate as **Eqns. 17 – 19** respectively thus:

Wall 1:
$$\frac{\partial}{\partial x_1}\left(k_{1x}(T_1)\frac{\partial T_1}{\partial x_1}\right)+\frac{\partial}{\partial y}\left(k_{1y}(T_1)\frac{\partial T_1}{\partial y}\right)=\frac{\partial\left(\rho_1 c_{p1}T_1\right)}{\partial t} \qquad \textbf{Eqn. 17}$$

Wall 2:
$$\frac{\partial}{\partial x_2}\left(k_{2x}(T_2)\frac{\partial T_2}{\partial x_2}\right)+\frac{\partial}{\partial y}\left(k_{2y}(T_2)\frac{\partial T_2}{\partial y}\right)=\frac{\partial\left(\rho_2 c_{p2}T_2\right)}{\partial t} \qquad \textbf{Eqn. 18}$$

Wall 3:
$$\frac{\partial}{\partial x_3}\left(k_{3x}(T_3)\frac{\partial T_3}{\partial x_3}\right)+\frac{\partial}{\partial y}\left(k_{3y}(T_3)\frac{\partial T_3}{\partial y}\right)=\frac{\partial\left(\rho_3 c_{p3}T_3\right)}{\partial t} \qquad \textbf{Eqn. 19}$$

2.1.1 Initial condition

Initially, the temperature in the wall is equal to the atmospheric temperature. Therefore, the initial conditions of each wall and the interface conditions are given in **Eqns. 20a, 20b** and **20c** respectively as follows:

$$t=0,\quad T_1=T_a \qquad 0\le x_1\le l_1,\quad 0\le y\le H, \qquad \textbf{Eqn. 20a}$$

$$t=0,\quad T_2=T_a \qquad l_1\le x_2\le l_2,\quad 0\le y\le H, \qquad \textbf{Eqn. 20b}$$

$$t=0,\quad T_3=T_a \qquad l_2\le x_3\le l_3,\quad 0\le y\le H, \qquad \textbf{Eqn. 20c}$$

2.1.2 The boundary conditions;

The boundary conditions of each wall and the interface conditions are given as follows. At the outer face where ***x = 0***, the heat that reaches the face by convection is equal to heat that leaves the face by conduction. Mathematically, this is stated in **Eqn. 21** as:

$$\text{at } t>0, \quad x=0, \quad -k_1\frac{\partial T_1}{\partial x_1}=h_o\left(T_1-T_a\right), \quad 0\le y\le H \qquad \textbf{Eqn. 21}$$

Similarly, at the inner face where $x = L$, the heat that reaches the face by convection is equal to heat that leaves the face by conduction. Mathematically, this is expressed in **Eqn. 22** as

$$\text{at } t>0, \quad x=l_1+l_2+l_3=L, \quad -k_3\frac{\partial T_3}{\partial x_3}=h_{in}\left(T_3-T_{in}\right), \quad 0\le y\le H \qquad \textbf{Eqn. 22}$$

The lower and upper boundaries of the system are insulated, therefore, there is no heat flow across the lower and upper boundaries of the system. Therefore, **Eqns. 23a, 23b** and **23c** are the lower and **Eqns. 24a, 24b,** and **24c** are the upper boundaries equations respectively

$$t>0, \quad y=0, \quad \frac{\partial T_1}{\partial y}=0, \quad 0\le x_1\le l_1 \qquad \textbf{Eqn. 23a}$$

$$t>0, \quad y=0, \quad \frac{\partial T_2}{\partial y}=0, \quad l_1\le x_2\le l_2 \qquad \textbf{Eqn. 23b}$$

$$t>0, \quad y=0, \quad \frac{\partial T_3}{\partial y}=0, \quad l_2\le x_3\le l_3 \qquad \textbf{Eqn. 23c}$$

$$t>0, \quad y=H, \quad \frac{\partial T_1}{\partial y}=0, \quad 0\le x_1\le l_1 \qquad \textbf{Eqn. 24a}$$

$$t>0, \quad y=H, \quad \frac{\partial T_2}{\partial y}=0, \quad l_1\le x_2\le l_2 \qquad \textbf{Eqn. 24b}$$

$$t>0, \quad y=H, \quad \frac{\partial T_3}{\partial y}=0, \quad l_2\le x_3\le l_3 \qquad \textbf{Eqn. 24c}$$

2.1.3 Interlayer conditions

Assuming perfect thermal contact at the interfaces, the temperature and the heat transfer in the respective walls must be the same at every point in between the walls giving rise to **Eqns. 25, 26, 27** and **28.**

$$t>0, \ T_1=T_2, \ 0\le x_1\le l_1 \qquad \textbf{Eqn. 25}$$

$$t>0, \ T_2=T_3, \ l_1\le x_2\le l_2 \qquad \textbf{Eqn. 26}$$

$$t>0, \ k_1\frac{\partial T_1}{\partial y}=k_2\frac{\partial T_2}{\partial y}, \quad 0\le x_1\le l_1 \qquad \textbf{Eqn. 27}$$

$$t>0, \ k_2\frac{\partial T_2}{\partial y}=k_3\frac{\partial T_3}{\partial y}, \quad l_1\le x_2\le l_2 \qquad \textbf{Eqn. 28}$$

2.2 Finite Difference Method

Before using finite difference method to solve each wall thermal model equations developed, the thermal model equations, **Eqns. 17, 18** and **19** were expanded to give **Eqns. 29, 30** and **31** respectively:

Wall 1: $$k_{1x}(T_1)\frac{\partial^2 T_1}{\partial x_1^2}+k_{1x}(T_1)\left(\frac{\partial T_1}{\partial x_1}\right)^2+k_{1y}(T_1)\frac{\partial^2 T_1}{\partial y^2}+k_{1y}(T_1)\left(\frac{\partial T_1}{\partial y}\right)^2=\frac{\partial\left(\rho_1 c_{p1}T_1\right)}{\partial t} \qquad \textbf{Eqn. 29}$$

Wall 2: $$k_{2x}(T_2)\frac{\partial^2 T_2}{\partial x_2^2}+k_{2x}(T_2)\left(\frac{\partial T_2}{\partial x_2}\right)^2+k_{2y}(T_2)\frac{\partial^2 T_2}{\partial y^2}+k_{2y}(T_2)\left(\frac{\partial T_2}{\partial y}\right)^2=\frac{\partial\left(\rho_2 c_{p2}T_2\right)}{\partial t} \qquad \textbf{Eqn. 30}$$

Wall 3: $$k_{3x}(T_3)\frac{\partial^2 T_3}{\partial x_3^2}+k_{3x}(T_3)\left(\frac{\partial T_3}{\partial x_3}\right)^2+k_{3y}(T_3)\frac{\partial^2 T_3}{\partial y^2}+k_{3y}(T_3)\left(\frac{\partial T_3}{\partial y}\right)^2=\frac{\partial\left(\rho_3 c_{p3}T_3\right)}{\partial t} \qquad \textbf{Eqn. 31}$$

Applying Finite Difference Method, **Eqn. 29 – 31** become **Eqn. 32 – 34** respectively:

Wall 1:
$$k_{1x}\left(T_1\right)_{i,j}^{n}\left(\frac{\left(T_1\right)_{i+1,j}^{n+1}-2\left(T_1\right)_{i,j}^{n+1}+\left(T_1\right)_{i-1,j}^{n+1}+\left(T_1\right)_{i+1,j}^{n}-2\left(T_1\right)_{i,j}^{n}+\left(T_1\right)_{i-1,j}^{n}}{2\Delta x_1^2}\right)$$
$$+k_{1x}\left(T_1\right)_{i,j}^{n}\left(\frac{\left(T_1\right)_{i+1,j}^{n+1}-\left(T_1\right)_{i-1,j}^{n+1}+\left(T_1\right)_{i+1,j}^{n}-\left(T_1\right)_{i-1,j}^{n}}{4\Delta x_1}\right)^2$$
$$+k_{1y}\left(T_1\right)_{i,j}^{n}\left(\frac{\left(T_1\right)_{i,j+1}^{n+1}-2\left(T_1\right)_{i,j}^{n+1}+\left(T_1\right)_{i,j-1}^{n+1}+\left(T_1\right)_{i,j+1}^{n}-2\left(T_1\right)_{i,j}^{n}+\left(T_1\right)_{i,j-1}^{n}}{2\Delta y_1^2}\right)$$
$$+k_{1y}\left(T_1\right)_{i,j}^{n}\left(\frac{\left(T_1\right)_{i+1,j}^{n+1}-\left(T_1\right)_{i-1,j}^{n+1}+\left(T_1\right)_{i+1,j}^{n}-\left(T_1\right)_{i-1,j}^{n}}{4\Delta y_1}\right)^2=\rho_1 c_{p1}\left(\frac{\left(T_1\right)_{i,j}^{n+1}-\left(T_1\right)_{i,j}^{n}}{\Delta t}\right) \qquad \textbf{Eqn. 32}$$

Wall 2:
$$k_{2x}\left(T_2\right)_{i,j}^{n}\left(\frac{\left(T_2\right)_{i+1,j}^{n+1}-2\left(T_2\right)_{i,j}^{n+1}+\left(T_2\right)_{i-1,j}^{n+1}+\left(T_2\right)_{i+1,j}^{n}-2\left(T_2\right)_{i,j}^{n}+\left(T_2\right)_{i-1,j}^{n}}{2\Delta x_2^2}\right)$$
$$+k_{2x}\left(T_2\right)_{i,j}^{n}\left(\frac{\left(T_2\right)_{i+1,j}^{n+1}-\left(T_2\right)_{i-1,j}^{n+1}+\left(T_2\right)_{i+1,j}^{n}-\left(T_2\right)_{i-1,j}^{n}}{4\Delta x_2}\right)^2$$
$$+k_{2y}\left(T_2\right)_{i,j}^{n}\left(\frac{\left(T_2\right)_{i,j+1}^{n+1}-2\left(T_2\right)_{i,j}^{n+1}+\left(T_2\right)_{i,j-1}^{n+1}+\left(T_2\right)_{i,j+1}^{n}-2\left(T_2\right)_{i,j}^{n}+\left(T_2\right)_{i,j-1}^{n}}{2\Delta y_2^2}\right)$$
$$+k_{2y}\left(T_2\right)_{i,j}^{n}\left(\frac{\left(T_2\right)_{i+1,j}^{n+1}-\left(T_2\right)_{i-1,j}^{n+1}+\left(T_2\right)_{i+1,j}^{n}-\left(T_2\right)_{i-1,j}^{n}}{4\Delta y_2}\right)^2=\rho_2 c_{p2}\left(\frac{\left(T_2\right)_{i,j}^{n+1}-\left(T_2\right)_{i,j}^{n}}{\Delta t}\right) \qquad \textbf{Eqn. 33}$$

$$k_{3x}\left(T_3\right)_{i,j}^{n}\left(\frac{\left(T_3\right)_{i+1,j}^{n+1}-2\left(T_3\right)_{i,j}^{n+1}+\left(T_3\right)_{i-1,j}^{n+1}+\left(T_3\right)_{i+1,j}^{n}-2\left(T_3\right)_{i,j}^{n}+\left(T_3\right)_{i-1,j}^{n}}{2\Delta x_3^2}\right)$$

$$+k_{3x}\left(T_3\right)_{i,j}^{n}\left(\frac{\left(T_3\right)_{i+1,j}^{n+1}-\left(T_3\right)_{i-1,j}^{n+1}+\left(T_3\right)_{i+1,j}^{n}-\left(T_3\right)_{i-1,j}^{n}}{4\Delta x_3}\right)^2$$

Wall 3: **Eqn. 34**

$$+k_{3y}\left(T_3\right)_{i,j}^{n}\left(\frac{\left(T_3\right)_{i,j+1}^{n+1}-2\left(T_3\right)_{i,j}^{n+1}+\left(T_3\right)_{i,j-1}^{n+1}+\left(T_3\right)_{i,j+1}^{n}-2\left(T_3\right)_{i,j}^{n}+\left(T_3\right)_{i,j-1}^{n}}{2\Delta y_3^2}\right)$$

$$+k_{3y}\left(T_3\right)_{i,j}^{n}\left(\frac{\left(T_3\right)_{i+1,j}^{n+1}-\left(T_3\right)_{i-1,j}^{n+1}+\left(T_3\right)_{i+1,j}^{n}-\left(T_3\right)_{i-1,j}^{n}}{4\Delta y_3}\right)^2=\rho_3 c_{p3}\left(\frac{\left(T_3\right)_{i,j}^{n+1}-\left(T_3\right)_{i,j}^{n}}{\Delta t}\right)$$

2.2.1 Initial condition

The initial temperature of the wall is equal to the atmospheric temperature. This is given in **Eqn. 35** as:

$$t=0,\ \left(T_1\right)_{i,j}^{0}=\left(T_2\right)_{i,j}^{0}=\left(T_3\right)_{i,j}^{0}=T_a \qquad i=0,1,2,...,N, \quad j=0,1,2,...,M \qquad \textbf{Eqn. 35}$$

2.2.2 Boundary condition

At the outer face where $x = 0$, the heat that reaches the face by convection is equal to heat that leaves the face by conduction. It can therefore be stated mathematically in **Eqn. 36** as

$$\text{if } n>0, \quad i=0, \quad -k_1\left(T_1\right)_{0,j}^{n}\left(\frac{\left(T_1\right)_{1,j}^{n}-\left(T_1\right)_{-1,j}^{n}}{2\Delta x_1}\right)=h_o\left(\left(T_1\right)_{0,j}^{n}-T_a\right), \quad j=1,2,3,...,N \qquad \textbf{Eqn. 36}$$

Similarly, at the inner face where $x = L$, the heat that reaches the face by convection is equal to the heat that leaves the face by conduction. It can also be stated mathematically in **Eqn. 36** as

$$\text{for } n>0, \quad i=N\Delta x_3, \quad -k_3\left(T_3\right)_{N,j}^{n}\left(\frac{\left(T_3\right)_{N,j}^{n}-\left(T_3\right)_{N-1,j}^{n}}{\Delta x_3}\right)=h_{in}\left(\left(T_1\right)_{N,j}^{n}-T_{in}\right), \quad j=1,2,3,...,N \qquad \textbf{Eqn. 37}$$

There will be no heat flow across the lower and upper boundaries of the system because the system is lagged, these conditions are indicated in **Eqns. 38a, 38b, 38c. 38d, 38e** and **38f**

$$n>0, \quad j=0, \quad \left(\frac{\left(T_1\right)_{i,1}-\left(T_1\right)_{i,-1}}{\Delta y}\right)=0, \quad i=0,1,2,3,...,\mathrm{N} \qquad \textbf{Eqn. 38a}$$

$$n>0, \quad j=0, \quad \left(\frac{\left(T_2\right)_{i,1}-\left(T_2\right)_{i,-1}}{\Delta y}\right)=0, \quad i=0,1,2,3,...,\mathrm{N} \qquad \textbf{Eqn. 38b}$$

$$n>0, \quad j=0, \quad \left(\frac{\left(T_3\right)_{i,1}-\left(T_3\right)_{i,-1}}{\Delta y}\right)=0, \quad i=0,1,2,3,...,\mathrm{N} \qquad \textbf{Eqn. 38c}$$

$$n>0,\quad j=M\Delta y,\quad \left(\frac{(T_1)_{i,1}-(T_i)_{i,-1}}{\Delta y}\right)=0,\quad i=0,1,2,3,...,\mathrm{N} \qquad \textbf{Eqn. 38d}$$

$$n>0,\quad j=M\Delta y,\quad \left(\frac{(T_2)_{i,1}-(T_2)_{i,-1}}{\Delta y}\right)=0,\quad i=0,1,2,3,...,\mathrm{N} \qquad \textbf{Eqn. 38e}$$

$$n>0,\quad j=M\Delta y,\quad \left(\frac{(T_3)_{i,1}-(T_3)_{i,-1}}{\Delta y}\right)=0,\quad i=0,1,2,3,...,\mathrm{N} \qquad \textbf{Eqn. 38f}$$

2.2.3 Interlayer condition

Assuming perfect thermal contact at the interfaces, the heat transfer and the temperature must be equal in the respective walls and must be the same at each point in between the walls, therefore, this is indicated in **Eqns. 39 – 42.**

$$n>0,\ (T_1)^n_{i,j}=(T_2)^n_{i,j},\quad i=N\Delta x_1=N\Delta x_2=N\Delta x_3 \qquad \textbf{Eqn. 39}$$

$$n>0,\ (T_2)^n_{i,j}=(T_3)^n_{i,j},\quad i=N\Delta x_1=N\Delta x_2=N\Delta x_3 \qquad \textbf{Eqn. 40}$$

$$n>0,\ k_1(T_1)^n_{i,j}\left(\frac{(T_1)^n_{i,j+1}-(T_1)^n_{i,j}}{\Delta y}\right)=k_2(T_2)^n_{i,j}\left(\frac{(T_2)^n_{i,j+1}-(T_2)^n_{i,j}}{\Delta y}\right),\quad i=N\Delta x_1=N\Delta x_2=N\Delta x_3 \qquad \textbf{Eqn. 41}$$

$$n>0,\ k_2(T_2)^n_{i,j}\left(\frac{(T_2)^n_{i,j+1}-(T_2)^n_{i,j}}{\Delta y}\right)=k_3(T_3)^n_{i,j}\left(\frac{(T_3)^n_{i,j+1}-(T_3)^n_{i,j}}{\Delta y}\right),\quad i=N\Delta x_1=N\Delta x_2=N\Delta x_3 \qquad \textbf{Eqn. 42}$$

3.0 Results and Discussions

The atmospheric temperature of 30 ^{0}C and 32 ^{0}C were considered as initial temperatures in determination of the heat transfer across the composite walls. The temperature is plotted against time as shown in **Figures 4 -6**, for the numerical simulations of the thermal models for the composite walls of the refrigerators. The effects of atmospheric temperature on the thermal performance of the system is investigated and discussed.

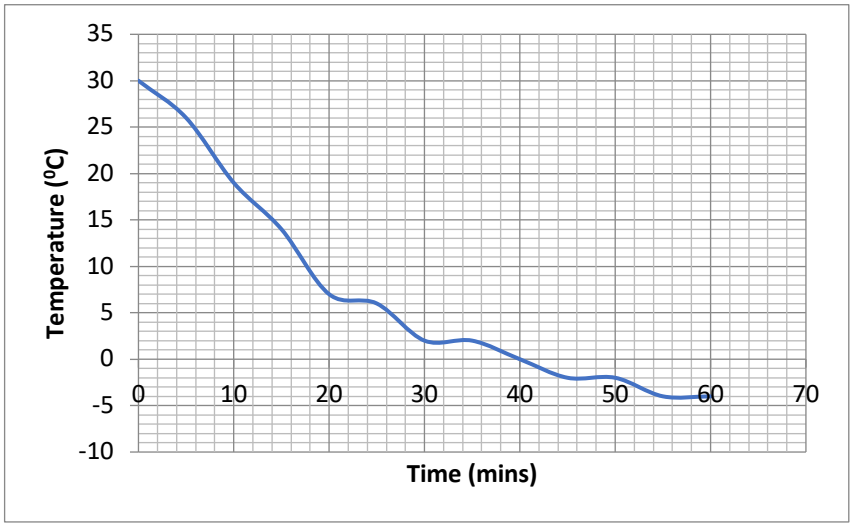

Figure 4: Temperature profile across the composite walls at ambient temperature of 30^{o}C

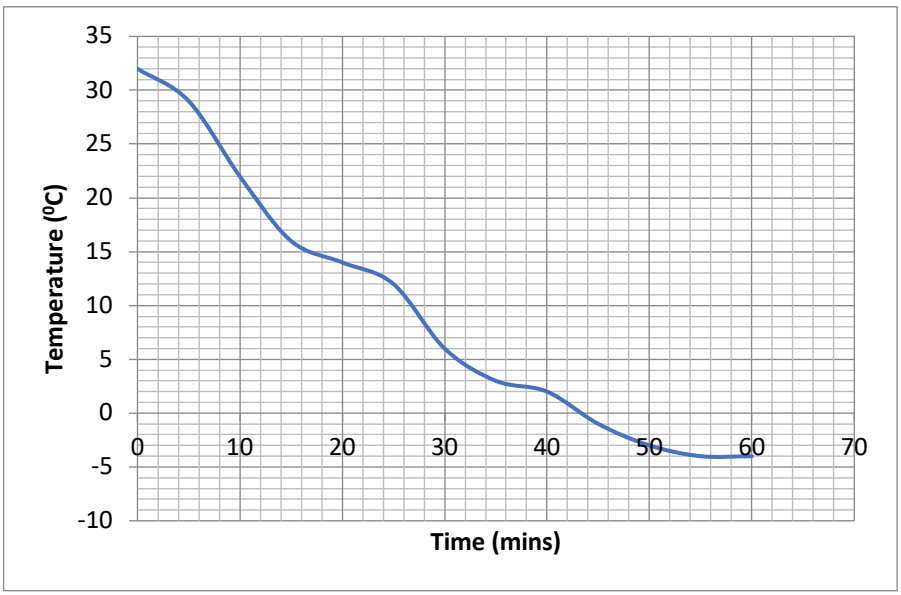

Figure 5: Temperature profile across the composite walls at ambient temperature of 32°C

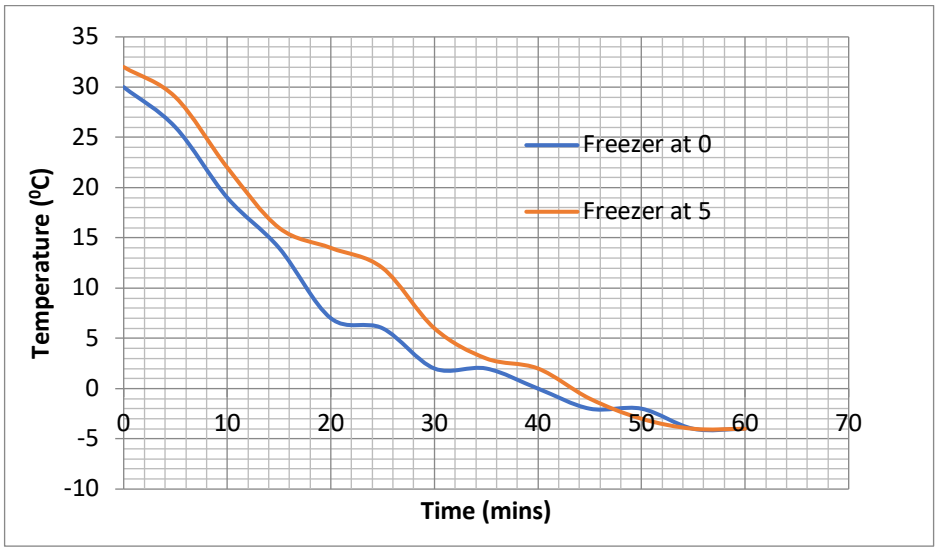

Figure 6: Effect of ambient temperature on the inner surface temperature profile of the internal steel in the composite wall

Figures 4 – 6 show the temperature profiles of the composite walls when the atmospheric temperature is 30°C and 32°C. Two general profiles were obvious from the figures. The first, T_a (= 30 °C) is a decreasing temperature for the time range. This trend is the same for all the composite walls. Although, the outcomes of these two different cases followed the same pattern, but they are different in magnitude due to different ambient temperatures. The second pattern that was observed in the figures is for wall that showed a reduction (monotonic decrease) in temperature from T_a (= 32 °C) to the steady state value of -5 ^{0}C. The variation in behavior between the two patterns could be attributed to the difference in atmospheric temperature. The external steel is subjected to higher temperature from the environment (atmosphere) therefore it is expected that the external wall required more time to reach steady state conditions. Due to the sandwiched insulator in between the internal and external steels, there is significant changes in gradient of the graphs which occur in the internal and external steels. However, the distribution of temperature across each wall is generally monotonically decreasing at all times until it becomes steady state conditions in the refrigerator. The Findings are in good agreements with those obtained by several authors (Zhang *et al* (2022); Salhi *et al* (2022); Wang, (2012))

Conclusions

In this work, two-dimensional thermal model equations for the heat conductions through composite walls of a refrigerator has been developed and solved using finite difference numerical method. The performance of this system under two ambient temperature was simulated for the composite walls. It can be concluded from the numerical simulation that the performance of the refrigerator is dependent on the ambient temperature, convective heat transfer coefficient, thicknesses of the composite walls, the thermal properties of the insulating material and the thermal properties of the metallic. Since the present work is limited to two-dimensional thermal modelling for the heat conductions through composite walls of the refrigerator, it is recommended that the work could still be extended to three-dimensional analysis and the heat and momentum transfer in the chamber of the refrigeration system could be carried out using computational fluid dynamic approach. This will assist in the all-inclusive simulations and analyses of the different aspect of the refrigerating system.

References

Aktacir M. A. (2011). Experimental Study of a multiple-purpose PV-refrigerator system, *Int. Journal of Physical Sciences*, 6(4), 746 – 757.

Biswas, O., Kandasamy, K., (2021). Development and Experimental Investigation of Portable Solar-powered Thermoelectric Cooler for Preservation of Perishable Foods. *International Journal of Renewable Energy Research.* 11(3), 1292 – 1303.

Chavan, P.; Sidhu, G.K.; Jaiswal, A.K. (2022). Performance Evaluation of Mobile Liquid Cooled Thermoelectric Refrigeration System for Storage-Cum-Transportation of Fruits and Vegetables. *Foods*, 11, 1896. https://doi.org/10.3390/ foods11131896

Ewert M K, Agrella M, Frahm J, Bergeron DJ, Berchowitz D. (1998). Experimental evaluation of a solar PV-refrigerator with Thermoelectric, Stirling and Vapor Compression Heat Pumps. *Proceedings of Solar*, ASES.

Hafeez, M.B., Krawczuk, M., Jamshed, W. et al. (2022). Improved finite element method for flow, heat and solute transport of Prandtl liquid via heated plate. *Sci. Rep.* 12, 19681, https://doi.org/10.1038/s41598-022-20332-2

Harvey A.B., (1990). *Study of an intermittent regenerative cycle for solar cooling, Ph.D. thesis*, University of Warwick, UK.

Hinotani K. et al, (1986). Development of a solar absorption refrigeration system, *ISES Solar World Congress*, Hamburg, pub. Pergammon.

Iloeje O.C., (1977). Parametric effects on the performance of a solar powered solid absorption refrigerator, *Solar Energy*, 40(3), 191-195.

Imam Osman Ahmed, Stoetjes, E.W., Kerkdijk, C., Stolk, A.L., (1986). Experience with a 13kW / 50 m^2 solar driven absorption refrigerator in the Sudan, *ISES Solar World Congress*, Hamburg, pub. Pergammon.

Kim D. S, and Ferreira I. C. (2008). Solar refrigeration options–a state-of-the art review. *Int. J. Refrig*., 31, 3 - 15.

Lawal, O., Chang, Z., (2021). Development of an effective TE cooler box for food storage. *Case Studies in Thermal Engineering*, 28, Dec 2021, 101564. DOI: 10.1016/j.csite.2021.101564

Midiani L P I, Subagia, I W A, Suastawa, I W, Sapteka, A A N G, Winarta, A. (2020). Preliminary investigation of performance and temperature distribution of thermoelectric cooler box with and without internal fan. *Journal of Physics: Conference Series*. 1450, 012088 IOP Publishing doi:10.1088/1742-6596/1450/1/012088

Mohamed A. E. and Samuel D.V. (2007). Performance and Economic Evaluation of Solar Photovoltaic Powered Cooling System for Potato Storage. *Agricultural Engineering International: the CIGR E Journal*. Manuscript EE 07 008. 200) Vol. IX.

Ren Y., Ogura H. (2021). Performance evaluation of off-grid solar chemical heat pump for cooling/heating, *Solar Energy,* 224, 1247-1259, https://doi.org/10.1016/j.solener.2021.06.046

Salhi J-E., Zarrouk T., Salhi M., Salhi N. (2022). Analysis of the surface state's influence on the thermohydraulic behavior of an incompressible fluid in convective laminar flow through a microchannel with corrugated surfaces, *EHEI J. Sci. Technol.* 2(2), 68-77

Saunier G.Y., Reddy T.A. (1986). Multi-fuel ice-making machine', *Asian Institute of Technology Report* No. 190, Bangkok, Thailand.

Sobamowo M. G., Ogunmola B. Y., Ojolo S. J., Oke D. B. (2012). Design and Development of a Dual Powered Refrigerator System with an Incorporated Solar Tracker. *Proceedings of the 4th 2012 International Conference on Engineering Research & Development*, University of Benin, Nigeria, Sept. 4 - 7.

Wang D. (2012). Analytical approach to predict temperature profile in a multilayered pavement system based on measured surface temperature data. *J. Transport. Eng.*, 138, 674–679.

Zhang Q., Dai G., Tang Y. (2022). Thermal Analysis and Prediction Methods for Temperature Distribution of Slab Track Using Meteorological Data. *Sensors*, 22, 6345. https://doi.org/10.3390/s22176345

(2023) ; http://www.jmaterenvironsci.com